Biochimie 175 (2020) 132–145

Contents lists available at ScienceDirect

Biochimie

journal homepage: www.elsevier.com/locate/biochi

Synthetic antimicrobial peptides: From choice of the best sequences to action mechanisms

Pedro F.N. Souza [a, *], Lidyane S.M. Marques [a], Jose T.A. Oliveira [a], Patrícia G. Lima [a], Lucas P. Dias [a], Nilton A.S. Neto [a], Francisco E.S. Lopes [a], Jeanlex S. Sousa [b], Ayrles F.B. Silva [a], Rômulo F. Caneiro [c], Jose L.S. Lopes [d], Márcio V. Ramos [a], Cleverson D.T. Freitas [a, **]

[a] Department of Biochemistry and Molecular Biology, Federal University of Ceará, Fortaleza, Ceará, CEP 60.440-554, Brazil
[b] Department of Physics, Federal University of Ceará, Fortaleza, Brazil
[c] Department of Fishery Engineering, Federal University of Ceará, Fortaleza, Brazil
[d] Institute of Physics, University of Sao Paulo, Sao Paulo, Brazil

ARTICLE INFO

Article history:
Received 26 January 2020
Received in revised form
16 May 2020
Accepted 30 May 2020
Available online 11 June 2020

Keywords:
Antibiofilm activity
Candida
Dermatophyte
Peptide design
SAMP

ABSTRACT

The emergence of antibiotic-resistant microbes has stimulated research worldwide seeking new biologically active molecules. In this respect, synthetic antimicrobial peptides (SAMPs) have been suggested to overcome this problem. Although there are some online servers that provide putative SAMPs from protein sequences, the choice of the best peptide sequences for further analysis is still difficult. Therefore, the goal of this paper is not to launch a new tool but to provide a friendly workflow to characterize and predict potential SAMPs by employing existing tools. Using this proposed workflow, two peptides (PepGAT and PepKAA) were obtained and extensively characterized. These peptides damaged microbial membranes and cell walls, and induced overproduction of reactive oxygen species (ROS). Both peptides were found to assume random coil secondary structure in aqueous solution, organic solvent, and upon binding to negatively charged lipid systems. Peptides were also able to degrade formed biofilms but not to prevent biofilm formation. PepGAT was not resistant to proteolysis, whereas PepKAA was resistant to pepsin but not to pancreatin. Furthermore, both presented no hemolytic activity against red blood cells, even at a 10-fold higher concentration than the antimicrobial concentration. The pipeline proposed here is an easy way to design new SAMPs for application as alternatives to develop new drugs against human pathogenic microorganisms.

1. Introduction

The 1940s was an important period for microbiology and drug development due to the release of the first antibiotic (penicillin) for clinical use. During the ensuing 50 years, microbe-mediated infectious diseases were under control in most countries, mainly developed ones. However, as a consequence of overuse and misuse of drugs, the number of resistant microbes has increased, making some conventional drugs ineffective [1]. Nowadays, there are many bacteria and fungi highly resistant to traditional drugs, such as erythromycin, tetracycline, chloramphenicol, fluconazole, itraconazole, and echinocandins. Thus, the continued misuse of antibiotics as the first choice to manage microbial infections is inappropriate and increases the risk of producing multiple microbial resistance to these drugs [2,3].

To face that global health threat, synthetic antimicrobial peptides (SAMPs) have emerged due to various advantages, such as potent activity, low production cost and no or very low toxicity [4,5]. Thus, many research groups have been seeking new SAMPs [6–8]. As a consequence, some free online servers have also been

* Corresponding author. Department of Biochemistry and Molecular Biology, Federal University of Ceará, Laboratory of Plant Defense Proteins, Av. Mister Hull, P.O. Box: 60451 Fortaleza, CE, Brazil.
** Corresponding author. Department of Biochemistry and Molecular Biology, Federal University of Ceará, Laboratory of Plant Proteases, Fortaleza, CE, Brazil.
E-mail addresses: pedrofilhobio@gmail.com (P.F.N. Souza), cleversondiniz@ufc.br (C.D.T. Freitas).

https://doi.org/10.1016/j.biochi.2020.05.016
0300-9084/

created to predict and characterize SAMPs [9,10].

By using those servers, it is possible to prospect for SAMPs from any protein sequence. Then, employing some criteria from natural antimicrobial proteins/peptides, such as positive net charge, hydrophobicity, helicity [11], and the Boman index [12], those servers can predict sequences with antimicrobial potential. The most important advantages of designing SAMPs from natural sequences are (1) gain of function, since SAMPs can present activities that were not present in the original model sequence [6,13,14]; and (2) reduction of toxicity and allergenicity, because during peptide design it is possible to remove these specific sequences. Recently, SAMPs have been designed from *Moringa oleifera* chitin-binding protein, *Mo*-CBP$_3$ [6], and 2S albumin from *Ricinus communis* seed cake, Rc-2S-Alb [8]. In both cases, peptides presented gain of function when compared to their original proteins. For instance, *Mo*-CBP$_3$ has no antibacterial activity and weak anticandidal activity, whereas its synthetic peptide (*Mo*-CBP$_3$-PepIII) exhibits antibacterial and anticandidal activity at concentrations as low as 2.2 μM [6]. Similarly, Rc-2S-Alb has no antifungal activity reported. However, peptides (*RcAlb*-PepI and *RcAlb*-PepII) derived from it exhibit antifungal activity at 9 μM [8].

The main drawback of using online servers to predict SAMPs is the huge list of peptides generated, making it hard to choose the best sequence for further analysis of biological activity. Therefore, the main goal of this work is to propose an easy and smooth workflow to help researchers seek new SAMPs from entire proteins by using existing tools. Employing this pipeline, it was possible to design and characterize two SAMPs and understand their action mechanism against bacteria and fungi. Besides this, their low hemolytic potential suggests they are suitable for clinical trials.

2. Materials and methods

2.1. Microorganisms

All tested yeasts belonged to the *Candida* genus, namely *C. albicans* (ATCC 10231), *C. parapsilosis* (ATCC 22019), *C. krusei* (ATCC 6258), and *C. tropicalis* (clinical isolate), whereas the filamentous fungi belonged to the *Trichophyton* genus, namely *T. mentagrophytes* and *T. rubrum*. The gram-positive bacteria tested were *Staphylococcus aureus* (ATCC 25923) and *Bacillus subtilis* (ATCC 6633), while the gram-negative bacteria were *Salmonella enterica* (ATCC 14028), *Enterobacter aerogenes* (ATCC 13048), *Pseudomonas aeruginosa* (ATCC 25619), *Klebsiella pneumoniae* (ATCC 10031) and *Escherichia coli* (ATCC 8739). All microorganisms were obtained from the Laboratory of Plant Toxins of the Department of Biochemistry and Molecular Biology of Federal University of Ceará (UFC).

2.2. Bioinformatics analyses

2.2.1. Prediction and characterization of antimicrobial peptides

To design the peptides, we applied a pipeline divided into four steps, summarized in Fig. 1. The first step was to choose a random protein sequence from the NCBI database (https://www.ncbi.nlm.nih.gov/). The protein chosen was a chitinase (NCBI accession number NP_181885.1) obtained from *Arabidopsis thaliana* [15]. In the second step, the chitinase sequence was analyzed using two free online servers: (1) dPABBs (http://ab-openlab.csir.res.in/abp/antibiofilm/protein.php), which is used to design peptides with antibiofilm activity [10]; and (2) CellPPD (http://crdd.osdd.net/raghava/cellppd/submission.php), which is used to design cell-penetrating peptides [9].

The peptides that had both antibiofilm and cell-penetrating action were selected and then characterized based on their predicted physico-chemical properties by using different online servers, such as positive net charge (at least +1), total hydrophobic ratio ranging from 40 to 60%, and Boman index (≤2.5) [12]. These criteria were evaluated using the Antimicrobial Peptide Database (APD3) tool (http://aps.unmc.edu/AP/design/design_improve.php) [16]. The pI (https://web.expasy.org/protparam/protpar-ref.html) [17], presence of cleavage sites (http://web.expasy.org/peptide_cutter/) [17], molecular mass (http://aps.unmc.edu/AP/); [18], and resistance to proteolysis (http://crdd.osdd.net/raghava/hlp/help.html) [19] were also assessed.

The peptides were blasted against the antimicrobial database (APD3, http://aps.unmc.edu/AP/) to evaluate the similarity with antibacterial and antifungal peptides experimentally tested [18], and the antibacterial and antifungal potential were predicted using the iAMPpred tool (http://cabgrid.res.in:8080/amppred/server.php) [20]. Additionally, some biological properties were predicted. The allergic potential was calculated using the antigenic prediction tool (http://imed.med.ucm.es/Tools/antigenic.pl) [21], while the hemolytic and toxic potentials were evaluated using HemoPI (http://crdd.osdd.net/raghava/hemopi/submitfreq.php?ran=44366); [22], and ToxinPred tools (http://crdd.osdd.net/raghava/toxinpred/design.php) [23], respectively.

2.2.2. Structural analyses

The helicity of antimicrobial peptides has been reported as an important characteristic for successful insertion in the membrane and then pore formation. Therefore, in the fourth step in the pipeline (Fig. 1), the 3D structures of the peptides were evaluated by simulation using the freely available PEP-FOLD online server (http://bioserv.rpbs.univ-paris-diderot.fr/services/PEP-FOLD/). The best models were chosen based on lowest sOPEP energy and highest Tm values, as defined by the PEP-FOLD server [24]. The analyses of the 3D structures were performed using the Py*Mol* Molecular Graphics System (version 1.7.4, Schrödinger, LLC) with the educational license [25]. In addition, the helicity of peptides was calculated using the program Rampage (http://mordred.bioc.cam.ac.uk/~rapper/rampage.php), the helix formation was evaluated by Ramachandran plotting [26], and wheel projection and hydrophobic moment were predicted using HeliQuest (http://heliquest.ipmc.cnrs.fr).

After all analyses cited above, two peptides from *A. thaliana* chitinase showed high potential as antimicrobials [GATIRAVNSR (PepGAT) and KAANRIKYFQ (PepKAA)]. Therefore, both were synthesized by the company GenOne (São Paulo, Brazil) and the quality and purity (≥95%) were assessed by reverse-phase high-performance liquid chromatography (RP-HPLC) and mass spectrometry, according to Dias et al. [8].

2.3. Biological assays

2.3.1. Antibacterial activity

The peptides were tested against *S. aureus*, *B. subtilis*, *S. enterica*, *E. aerogenes*, *P. aeruginosa*, *K. pneumoniae* and *E. coli* by applying the method described by Oliveira et al. [6]. After 24 h, the bacterial growth was measured by absorbance at 600 nm using an automated microplate reader (Epoch, BioTek Instruments Inc., USA). The antibiotic ciprofloxacin was used as a positive control, whereas the negative control was 0.15 M NaCl containing 5% DMSO (NaCl-DMSO solution), which was also used to dissolve the peptides. Synthetic peptides were tested in concentrations ranging from 50 to 0.39 μg mL^{-1} (1:2 serial dilutions). All assays were repeated three times and the results are expressed as mean ± standard deviation.

2.3.2. Anticandidal activity

Aliquots (100 μL) of *C. albicans*, *C. parapsilosis*, *C. krusei*, and *C. tropicalis* cell suspensions (2.5 x 10^3 CFU/mL) in potato dextrose

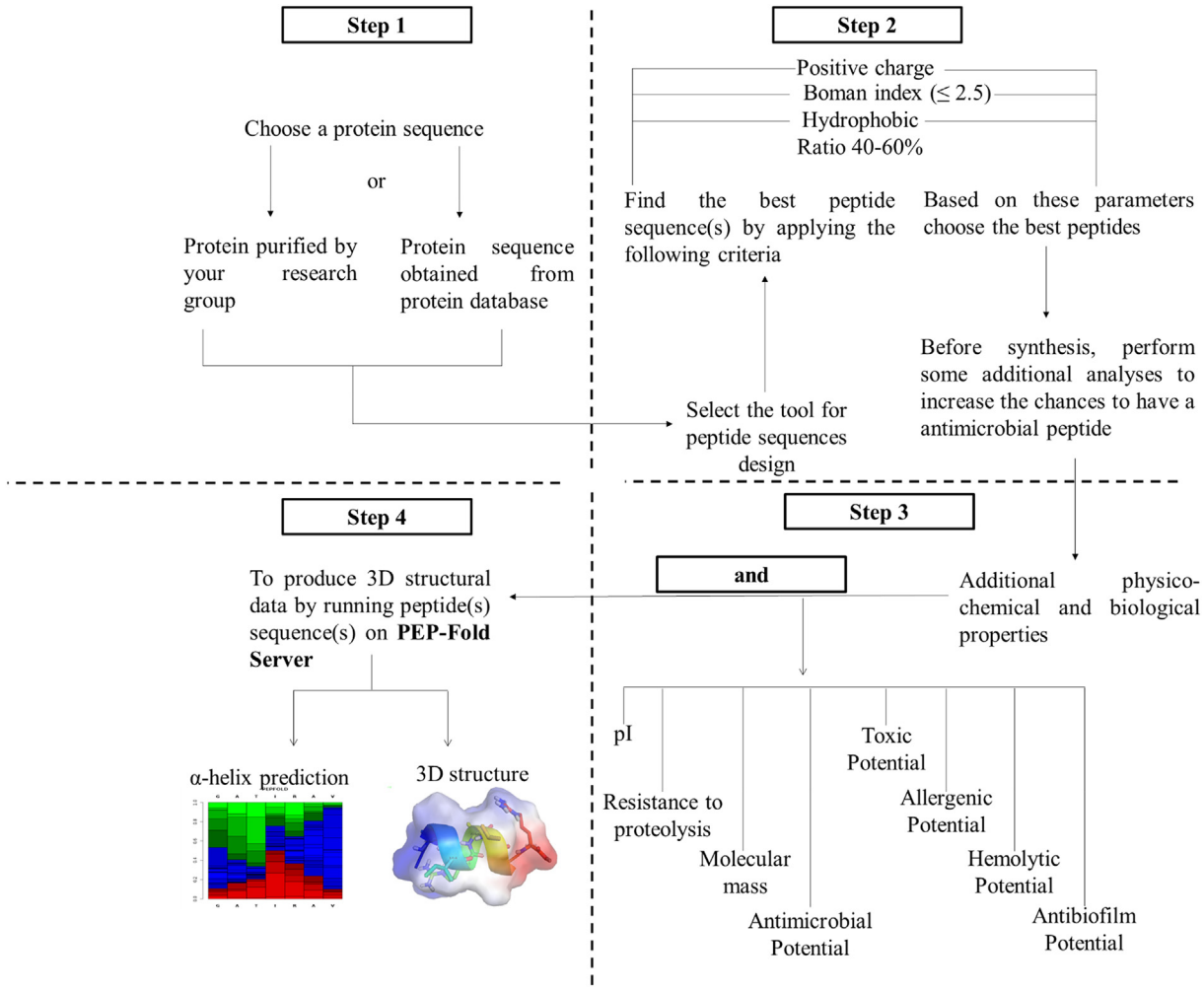

Fig. 1. Pipeline to design SAMPs based on any protein sequence. The first step is to choose a protein sequence. After that, select an online server to predict SAMPs. The third and fourth steps include characterizing all peptides using several bioinformatics tools. The peptides that presented all characteristics of natural antimicrobial peptides are then selected for further synthesis and *in vitro* assays.

broth medium (PDB) were mixed and incubated with 100 μL of peptides at different concentrations (50–0.39 μg mL^{-1}, in NaCl-DMSO solution) [6]. After 24 h, yeast growth was measured by absorbance at 600 nm using an automated microplate reader (Epoch, BioTek Instruments Inc., USA). Nystatin was used as the positive control and a NaCl-DMSO solution was used as the negative control (100% growth). All assays were repeated three times and the results are shown as mean ± standard deviation.

2.3.3. Antidermatophytic activity

First, inoculum suspensions of *T. mentagrophytes* and *T. rubrum* were prepared and the concentration was adjusted following the method described by Lopes et al. [27]. The assays were performed in microtiter plates with 96 flat-bottomed wells, as indicated by the Clinical and Laboratory Standards Institute (CLSI) M38-A2 method [28]. Peptides (100 μL), at concentrations ranging from 50 to 0.39 μg mL^{-1}, were added to 100 μL of *T. mentagrophytes* or *T. rubrum* microconidial suspension (OD. 0.1 at 600 nm). Griseofulvin (1 mg mL^{-1}), a commercial antifungal drug, was used as positive control for inhibition of fungal growth, while a NaCl-DMSO solution was used as negative control (100% growth). The mixture was incubated at 28 °C and the microconidial germination was monitored at 620 nm using an automated microplate reader (Model Elx800, Bio-Tek Instruments). All assays were repeated three time and the results are expressed as mean ± standard deviation.

2.3.4. Antibiofilm assay

The antibiofilm assays against bacteria and yeasts were performed according to the method described by Dias et al. [8]. The same controls and peptide concentrations used in the planktonic assays (sections 2.3.1. and 2.3.2) were applied in the biofilm assays. All assays were repeated three times and the results are expressed as mean ± standard deviation.

2.4. Action mechanism

2.4.1. Structural studies of peptides by circular dichroism

Circular dichroism (CD) spectroscopy [29] was employed to study possible conformational changes of PepGAT (50 μg. mL^{-1}) and PepKAA (50 μg. mL^{-1}) in the presence of the organic solvent 2,2,2-trifluoroethanol (TFE, 50%), when compared to 10 mM sodium phosphate buffer (pH 7.0). The CD spectra of both peptides were also recorded in the presence of model membranes composed of 20 mM sodium dodecyl sulfate (SDS), 20 mM N-hexadecyl-N-N′-dimethyl-3-ammonio-1-propane-sulfonate (HPS), large unilamellar vesicles of 1-palmitoyl-2-oleoyl-sn-glycero-3-phosphocholine (POPC) or 1-palmitoyl-2-oleoyl-sn-glycero-3-

phosphoglycerol (POPG), all used at a 1:50 peptide-to-lipid molar ratio. The analyses were performed using a J-815 spectropolarimeter (Jasco Inc., Japan) over the wavelength range from 280 to 190 nm, in 1 nm steps, at an average of 9 accumulations, using a 0.1 cm path-length cylindrical Suprasil quartz cuvette (Hellma), at 25 °C.

All CD data were processed using the CDtoolX [30] software, which included averaging the individual scans, subtraction of the corresponding baseline spectra, smoothing with a Savitzky–Golay filter, zeroing over the range from 267 to 270 nm, and final spectra conversion to delta epsilon units using mean residue weights of 116 and 137.6, to PepGAT and PepKAA, respectively.

2.4.2. Pore formation, reactive oxygen species (ROS) induction, and cell wall damage

To assess the possible mechanism of action of the peptides, some microorganisms tested were evaluated for pore formation on the cell membrane by using propidium iodide (PI). The induction of overproduction of ROS by peptides was detected using 2′,7′-dichlorofluorescein diacetate (DCFH-DA). In both assays, PI and DCFH-DA were incubated with the control and treated cells at 37 °C for 30 min in the dark, and then cells were washed three times with 0.15 M NaCl to remove the background. The images were taken using a fluorescent microscope (Olympus System BX 60: excitation wavelengths of 490 nm (PI) and 488 nm (DCFH-DA); emission wavelength of 525 nm) [8].

Two advanced microscopy techniques were employed to observe possible cell morphological alterations. Scanning electron microscopy (SEM) was applied to visualize the damage caused by peptides to the morphology of *T. mentagrophytes* microconidia, following the method described by Oliveira et al. [6]. In turn, the antibacterial and anticandidal activities of peptides were assessed by atomic force microscopy (AFM), according to Freitas et al. [31].

2.4.3. Interaction with chitin

The interaction of PepGAT and PepKAA with chitin was tested by affinity chromatography, as described by Lima et al. [32]. PepGAT and PepKAA (1 mg mL^{-1}) were loaded in a chitin column previously equilibrated with the NaCl-DMSO solution. The non-retained peak was eluted with the same solution used to equilibrate the column, while the retained peak was eluted sequentially with acetic acid, HCl or NaOH (all at 0.1 M), using a 0.5 mL min^{-1} flow rate. The elution of peptides was monitored at 230 nm using an automated absorbance reader (Epoch, BioTek Instruments, Inc., USA).

2.5. Digestibility and hemolytic potential

The peptides (0.5 mg mL^{-1}) were treated with a simulated gastric fluid (SGF: 0.034 M NaCl, 0.07% HCl and pepsin at 3.2 mg mL^{-1}) or simulated intestinal fluid (SIF: 0.05 M potassium phosphate and pancreatin at 10 mg mL^{-1}) for 2 s, 5 min, and 2 h, at 37 °C [8]. The intact and digested peptide samples (5 μL) were loaded in a reverse-phase C-18 nanocolumn (0.075 × 100 mm) coupled to a nanoACQUITY system, and the eluted material was analyzed in a hybrid mass spectrometer (ESI-Q-ToF) (Synapt HDMS, Waters Corp, MA, USA).

To evaluate the hemolytic potential, the peptides (50, 100, 250, and 500 μg mL^{-1}) were incubated with rabbit red blood cells for 1 h at 37 °C [8]. The protocol was approved by the Institutional Committee for Care and Use of Laboratory Animals of Federal University of Ceará.

3. Results

3.1. Selection and in silico characterization of peptides

As depicted in Fig. 1, the first step to design SAMPs is the choice of a protein sequence. Here, we selected a random protein sequence from the NCBI database (NP_181885) to test whether our workflow would work well. After the choice of protein sequence, the next step was to select the servers (Fig. 1). The servers dPABBs and CellPPD, which are used to design antibiofilm and cell-penetrating peptides, respectively, were used because they provide additional characterization of peptides compared to other servers [9,10].

Although peptides with different sizes can be generated by the dPABBs and CellPPD servers, short peptides are desired. Therefore, only peptides with ten amino acid residues were chosen here. After analyzing the results, both dPABBs (Table S1) and CellPPD (Table S2) generated 300 peptide sequences with ten amino acids. Out of 300 peptides generated by dPABBs, only 15 were predicted to be active against biofilms, whereas only three predicted by CellPPD were cell-penetrating. After careful evaluation, only two peptide sequences were both active against biofilms and had cell-penetration ability. Therefore, these two peptides [GATIRAVNSR (PepGAT) and KAANRIKYFQ (PepKAA)] were characterized and evaluated regarding antimicrobial potential.

Some bioinformatics tools were used to characterize PepGAT and PepKAA based on their physico-chemical and biological properties (Tables 1 and 2, respectively). Both peptides are cationic [PepGAT (+2) and PepKAA (+3)], have a good hydrophobic ratio (40%), and low Boman index (≤2.5), which are essential features for antimicrobial activity (Table 1) [11]. Indeed, the bioinformatics analyses predicted that the peptides would have antifungal potentials of 60 and 89%, whereas the antibacterial potentials were 77 and 60% for PepGAT and PepKAA, respectively (Table 2). Accordingly, when blasted against the database of experimentally tested antimicrobial peptides (APD, http://aps.unmc.edu/AP/), PepGAT had higher similarity with antibacterial peptides. On the other hand, PepKAA had higher similarity with antifungal peptides (Table S3).

In general, both peptides were predicted to contain a short helix secondary structure. However, the helix in PepGAT presented two turns, whereas PepKAA had one and a half turns (Fig. 2). These

Table 1
Some physicochemical properties of the synthetic peptides PepGAT and PepKAA.

Properties	PepGAT	PepKAA
Sequence	GATIRAVNSR	KAANRIKYFQ
[a] pI	12.00	10.29
[a] Calculated molecular mass (Da)	1044.18	1238.44
[b] Experimental molecular mass (Da)	1044.90	1239.00
[c] Boman index	2.19	2.28
[c] Hydrophobic ratio (%)	40	40
[d] Hydrophobic moment (μH)	0.275	0.398
[c] Net Charge	+2	+3
[e] Ramachandran Plot (%)	98	75
[f] Tm	0.360	0.414
[f] sOPEP	−7.39	−18.18

[a] pI and molecular mass were calculated using ProtParam (https://web.expasy.org/protparam/).
[b] Data obtained by mass spectrometry.
[c] Data generated by the Antimicrobial Peptide Database (APD3, http://aps.unmc.edu/AP/prediction/prediction_main.php).
[d] Hydrophobic moment was calculated using HeliQuest (http://heliquest.ipmc.cnrs.fr).
[e] Calculated using Rampage (http://mordred.bioc.cam.ac.uk/~rapper/rampage.php).
[f] Calculated using PepFOLD 3.0 (http://mobyle.rpbs.univ-paris-diderot.fr/cgi-bin/portal.py#forms::PEP-FOLD).

Table 2
Some properties of the synthetic peptides PepGAT and PepKAA obtained by bioinformatics.

Properties	PepGAT	PepKAA
[a]CPP	Yes	Yes
[b]Antibiofilm active	Yes	Yes
[c]Allergic Potential	No	No
[d]Hemolytic Potential (%)	5	4
[e]Toxic Potential	Non-toxic	Non-toxic
[f]Antimicrobial Potential (%)		
Antifungal	60	89
Antibacterial	77	60
[g]Cleavage sites		
Trypsin (high pH)	Yes	Yes
Pepsin (pH = 1.3)	Yes	No
Pepsin (pH > 2)	Yes	No
[h]Half-life	0.879	1.115
[i]Stability	Normal	High

[a] CPP (Cell Penetrating Peptide) capacity was calculated using the CellPPD tool (http://crdd.osdd.net/raghava/cellppd/multi_pep.php).
[b] The antibiofilm action was assessed using the dPABBs tool (http://ab-openlab.csir.res.in/abp/antibiofilm/protein.php).
[c] The allergic potential was calculated using the Antigenic Prediction tool (http://imed.med.ucm.es/Tools/antigenic.pl).
[d] The hemolytic potential was calculated by HemoPI tool (http://crdd.osdd.net/raghava/hemopi/submitfreq.php?ran=44366).
[e] The toxin potential was calculated using the ToxinPred (http://crdd.osdd.net/raghava/toxinpred/design.php).
[f] The antimicrobial potential was calculated using the iAMPpred tool (http://cabgrid.res.in:8080/amppred/).
[g] The cleavage sites was analyzed using the Peptide Cutter (http://web.expasy.org/peptide_cutter/).
[h] The half-life in seconds was calculated using the Half Life Prediction tool (http://crdd.osdd.net/raghava/hlp/help.html), which predicts the proteolytic activity in the intestinal-like environment.
[i] Stability was calculated using the Half Life Prediction tool (http://crdd.osdd.net/raghava/hlp/help.html). Half-life < 0.1 s means low stability; half-life from 0.1 to 1.0 s means normal stability; half-life > 1.0 s means high stability.

differences were corroborated by the Ramachandran plot (Table 1), where PepGAT had 98% favorable regions for helix formation and PepKAA had 75% (Table 1). The helical wheel projection analyses revealed more features about both peptides. Usually, a wheel projection is expected to show a helix formed by hydrophobic or apolar amino acids concentrated on one side of the helix, with polar amino acids on the other side. That was not of the case of PepGAT and PepKAA (Fig. S1). The wheel diagrams lead to the conclusion that neither PepGAT nor PepKAA have well-defined segregation of polar/charged and lipophilic faces, which means their α-helices do not look to be amphiphilic. The low hydrophobic moment for both peptides [PepGAT (0.275 μH) and PepKAA (0.398 μH)] can be the basis of their reduced antimicrobial action in comparison to other amphiphilic α-peptides, as it will be discussed further.

The electrostatic map revealed a small negatively charged region (red) and a large positively charged region (blue) in both peptides, mainly by the presence of two arginine (R) residues and one arginine and two lysine (K) residues, respectively, in PepGAT and PepKAA (Fig. 2). Besides this, it is possible to suggest the amino acid residues involved in possible antimicrobial activity: for PepGAT: Ala_2, Arg_5, Ala_6, Val_7, and Arg_{10}; while for PepKAA: Lys_1, $Ala_{2\text{-}3}$, Arg_5, Ile_6 and Lys_7. Those amino acids are important for antimicrobial activity because they can have two types of interaction with the cell membrane: (1) electrostatic, in which an attraction force drives peptide-membrane interaction; and (2) hydrophobic/apolar, involved in peptide insertion in the membrane [11].

Because several bioinformatics tools predicted that both PepGAT and PepKAA were cationic, had a good hydrophobic ratio and low Boman index, exhibited helix secondary structures as well as antibiofilm, cell-penetrating, antifungal and antibacterial activities, they were synthetized for further *in vitro* antimicrobial assays. The PepGAT and PepKAA exhibited theoretical molecular masses of 1044.18 Da and 1238.44 Da, respectively (Table 1), which were confirmed by mass spectrometry (MS). For both peptides, MS analyses showed two peaks, one monoprotonated and the other diprotonated (Fig. S2). The RP-HPLC profile of both peptides confirmed the samples' purity (Fig. S2, inserts).

3.2. CD spectra in the presence of different solvents and model membranes

The conventional CD spectra of PepGAT and PepKAA in aqueous solution (Fig. 2, black lines) presented a major negative peak centered near 195 nm region, which is typical of random coil structures, commonly assumed by short peptides. However, in the presence of 50% TFE (Fig. 2, red lines), an organic solvent, the CD spectra of both peptides were slightly changed, showing a slight alteration in the secondary structure, but still suggesting the presence of random coil structures (Fig. 2).

CD spectra of PepGAT and PepKAA when incubated with HPS (Fig. 2, blue lines) or POPC vesicles (Fig. 2, purple lines), which have zwitterionic characteristics, were similar to those in aqueous solvent, indicating no interaction. However, a slight change in the structure of the peptides, quite similar to that observed in TFE, was observed when membrane models containing a negative charge density on the surface (POPG vesicles or SDS systems) were used (Fig. 2, silver and green lines).

3.3. Antimicrobial assays and action mechanism

3.3.1. Antibacterial activity

The antibacterial assay revealed that both peptides were not active, even at the highest concentration tested (50 μg. mL^{-1}), against *E. aerogenes, E. coli,* and *P. aeruginosa* (Table 3). However, different results were observed against *K. pneumoniae*, *S. aureus*, *B. subtilis,* and *S. enterica* (Table 3). PepKAA was much less effective than PepGAT, presenting 8, 5, 5, and 4% inhibition, whereas PepGAT showed 25, 35, 31 and 80% inhibition against, respectively, *K. pneumoniae*, *S. aureus*, *B. subtilis,* and *S. enterica* (Table 3).

To understand the mechanism of the antibacterial activity of PepGAT (50 μg. mL^{-1}), *S. enterica* was chosen as a model. AFM images confirmed that control cells presented a typical bacillus-like form, with no cracks, scars or any other damage to the cell wall (Fig. 3). In contrast, the PepGAT-treated cells had severe damages and morphological alterations of the membrane, such as membrane protrusion and evagination (Fig. 3). This severe membrane damage also resulted in the loss of internal content (Fig. 3). Interestingly, the action of PepGAT on *S. enterica* led to uneven cell surface and loss of internal content, resulting in a reduction of cell volume (Fig. 3).

In addition, PepGAT induced pore formation on the cell membrane of *S. enterica,* which was observed by the propidium iodide (PI) uptake by *S. enterica* cells after contact with PepGAT (Fig. 4). The control cells, with intact membranes, showed no fluorescence, indicating no PI uptake (Fig. 4). The ability of PepGAT to induce pores on the *S. enterica* membrane corroborates the prediction of being a cell-penetrating peptide (Table 2). Additionally, PepGAT did not induce any ROS formation in *S. enterica* cells (Fig. 4).

3.3.2. Antifungal activity

The antifungal potential of peptides was tested against pathogenic dermatophytes and yeasts to humans. Antidermatophytic activity was evaluated against *T. mentagrophytes* and *T. rubrum*. Only PepKAA using the highest concentration tested (50 μg. mL^{-1}) was active, inhibiting *T. mentagrophytes* microconidial germination

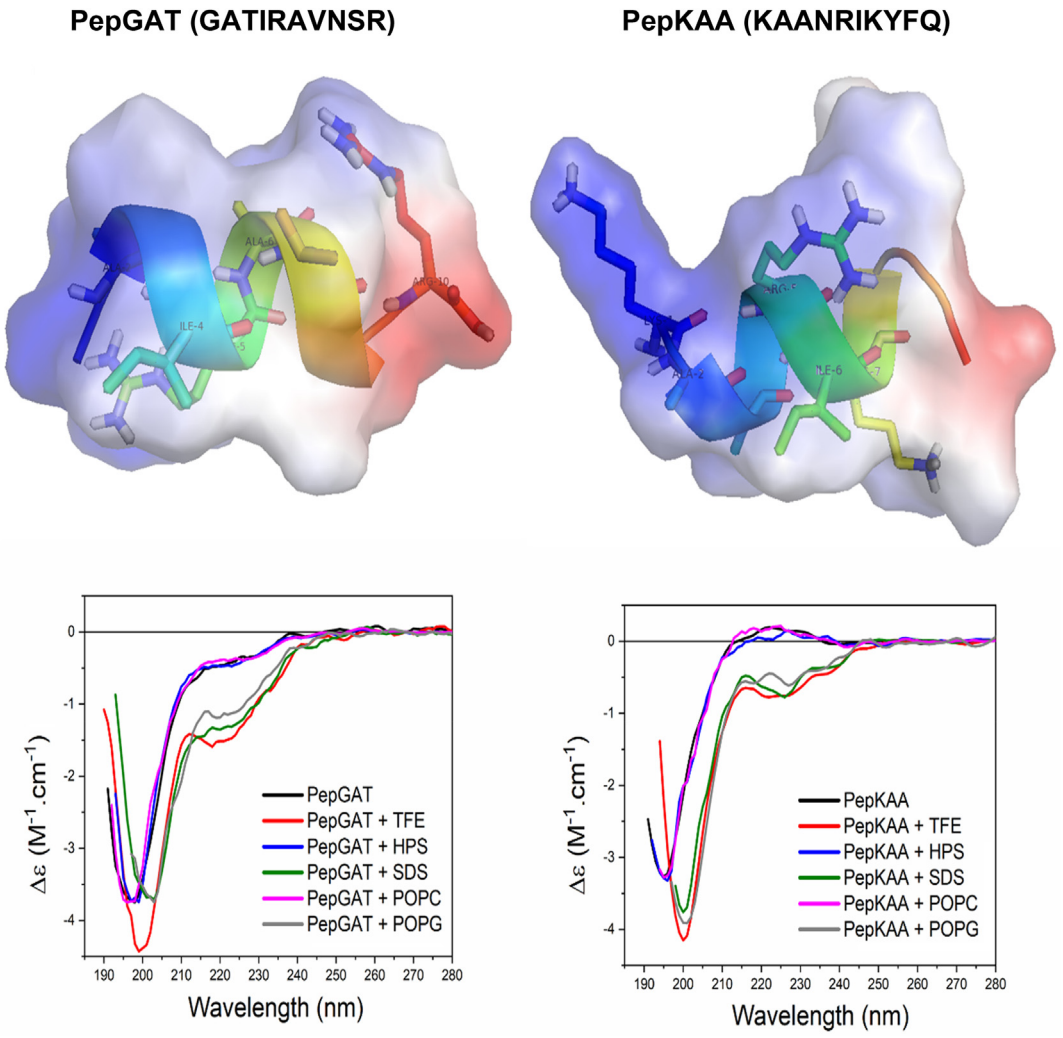

Fig. 2. 3D models and CD analyses of PepGAT and PepKAA. 3D Models were obtained using the PEPFold server and are presented in cartoon (main chain), stick (side chains) and surface representations. Blue and red surfaces represent positively and negatively charged amino acids, respectively. CD analyses were performed in 10 mM sodium phosphate buffer (pH 7.0), in TFE (50%) or in the presence of different membrane models (HPS, SDS, POPC and POPG).

by 90%, whereas *T. rubrum* was barely sensitive to both peptides (Table 3).

SEM images revealed control microconidia of *T. mentagrophytes* with healthy shape, with no cracks, damage, or altered morphology (Fig. 3). However, PepKAA treatment caused severe damage, such as loss of internal content, which is indicative of membrane pore formation (Fig. 3). The cell morphology was dramatically altered, with malformation, depressions, reduced cell volume, presence of warts and rougher surface (Fig. 3). Fluorescence analysis showed no PI uptake by control microconidia, confirming the cell membrane integrity (Fig. 4). However, PepKAA-treated microconidia presented red fluorescence, indicating PI uptake, corroborating the results of SEM, where severe membrane damage was observed (Fig. 3). Also, PepKAA was able to induce ROS overproduction (Fig. 4), which is indicative of oxidative stress in the fungus, compared to the control (Fig. 4).

3.3.3. Anticandidal activity

The anticandidal activity was tested against four species of the *Candida* genus (Table 3). Among them, *C. parapsilosis* and *C. tropicalis* were not affected by either peptide. In contrast, PepGAT and PepKAA (both at 50 μg. mL^{-1}) inhibited, respectively, the growth of *C. albicans* (40%) and *C. krusei* (80%) (Table 3). The action mechanisms of PepGAT and PepKAA against *C. albicans* and *C. krusei* were evaluated by AFM (Fig. 3). The control *C. albicans* had no cracks, scars, or any damage to the cell membrane (Fig. 3). However, PepGAT induced some damages, such as loss of cytoplasmic content, which can be seen around the cells (Fig. 3, white arrows). The control had ovoid and spherical cells (Fig. 3), while the PepGAT-treated cells lost this morphology, presenting extended tube-like forms, which is indicative of cell stress caused by treatment (Fig. 3).

AFM images also revealed that *C. krusei* cells suffered some damages after treatment with PepKAA (Fig. 3). Controls looked normal, presenting smooth surface, no cracks and spherical shape (Fig. 3). In contrast, all PepKAA-treated *C. krusei* cells presented damages and altered morphology, which likely led to death (Fig. 3). The damages caused by PepKAA were particularly evident, with cracks and scars crossing over the cells (Fig. 3, white arrows). Also, it was possible to see depressions like cavities in cells, indicating damage to cell wall and membrane. Besides that, it is important to mention the changes presented in Fig. 3, where cells were severely damaged and wrinkled, with signs of loss of internal content and dead cell fragments over other ones. In addition, both PepGAT and

Table 3
Antimicrobial activity of synthetic peptides PepGAT and PepKAA.

Microorganisms	% of inhibition	
	PepGAT	PepKAA
Bacteria	**50 μg mL^{-1}**	**50 μg mL^{-1}**
K. pneumoniae	25 ± 0.002	8 ± 0.032
S. aureus	35 ± 0.281	5 ± 0.018
B. subtilis	31 ± 0.009	5 ± 0.010
S. enterica	80 ± 0.023	4 ± 0.012
E. aerogenes	NA	NA
E. coli	NA	NA
P. aeruginosa	NA	NA
Yeast		
C. albicans	40 ± 0.221	NA
C. krusei	NA	80 ± 0.321
C. parapsilosis	NA	NA
C. tropicalis	NA	NA
Filamentous Fungus		
T. mentagrophytes	NA	90 ± 0.029
T. rubrum	5 ± 0.021	15 ± 0.001

NA = No activity.

PepKAA were able to induce pore formation, measured through PI uptake by cells, corroborating the damage visualized in the membrane by AFM analysis (Fig. 4). Although with low intensity, ROS overproduction in candida cells was also detected after treatment with peptides (Fig. 4).

3.4. Antibiofilm activity

Both peptides were predicted as having antibiofilm activity (Table 2), and this was used as a threshold to select them. Based on the results with planktonic cells, we decided to test the antibiofilm activity of PepGAT against *S. enterica* and PepKAA against *C. krusei* (Table 3, Figs. 3 and 4). The antibiofilm activity of peptides was tested by the ability to inhibit biofilm formation and to degrade previously formed biofilms. Both peptides were able to degrade existing biofilms but had no action on biofilm formation (Table 4). PepGAT was able to degrade 37% of the formed biofilms of *S. enterica*, while at the same concentration the antibiotic ciprofloxacin only degraded these films by 22%. PepGAT presented antibiofilm activity 68% higher than ciprofloxacin (Table 4). The ability of PepKAA to degrade formed biofilms of *C. krusei* was four times higher than the antifungal nystatin at the same concentration (Table 4). At 50 μg mL^{-1}, PepKAA degraded 40% of formed *C. krusei* biofilms, whereas nystatin only degraded 10% (Table 4).

3.5. Chitin-binding assay

Because PepGAT and PepKAA showed different selectivity to fungi and bacteria, a new assay was performed to study if they could interact with chitin, which is a main compound of fungal cell walls (Fig. 5). PepGAT did not interact with the chitin column, being eluted as non-retained peak, while PepKAA was strongly retained and eluted from the chitin column only after 0.1 M NaOH (Fig. 5). This result may explain, at least in part, why PepKAA was more active against fungi than PepGAT.

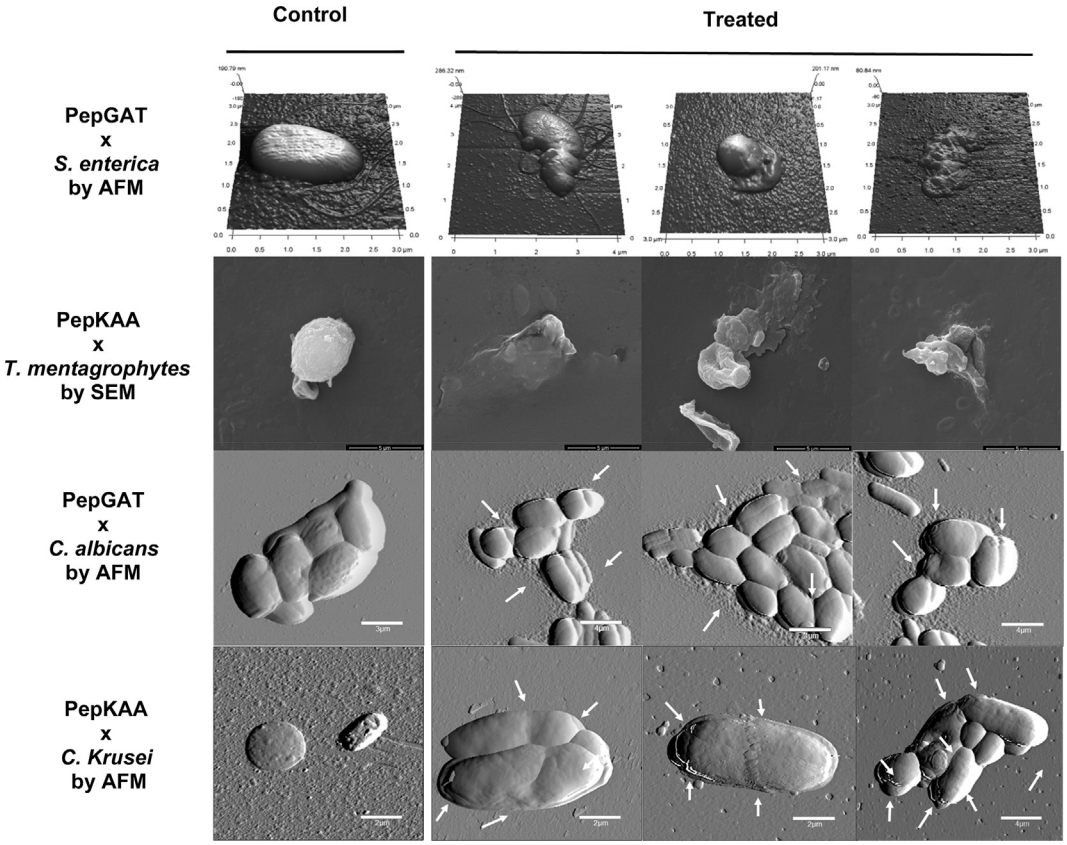

Fig. 3. Microscopic analyses showing alterations in the cell surface of different microorganisms after incubation with PepGAT and PepKAA. Both peptides were used at 50 μg. mL^{-1}. NaCl-DMSO solution was used as control. White arrows indicate damage in the candida cells.

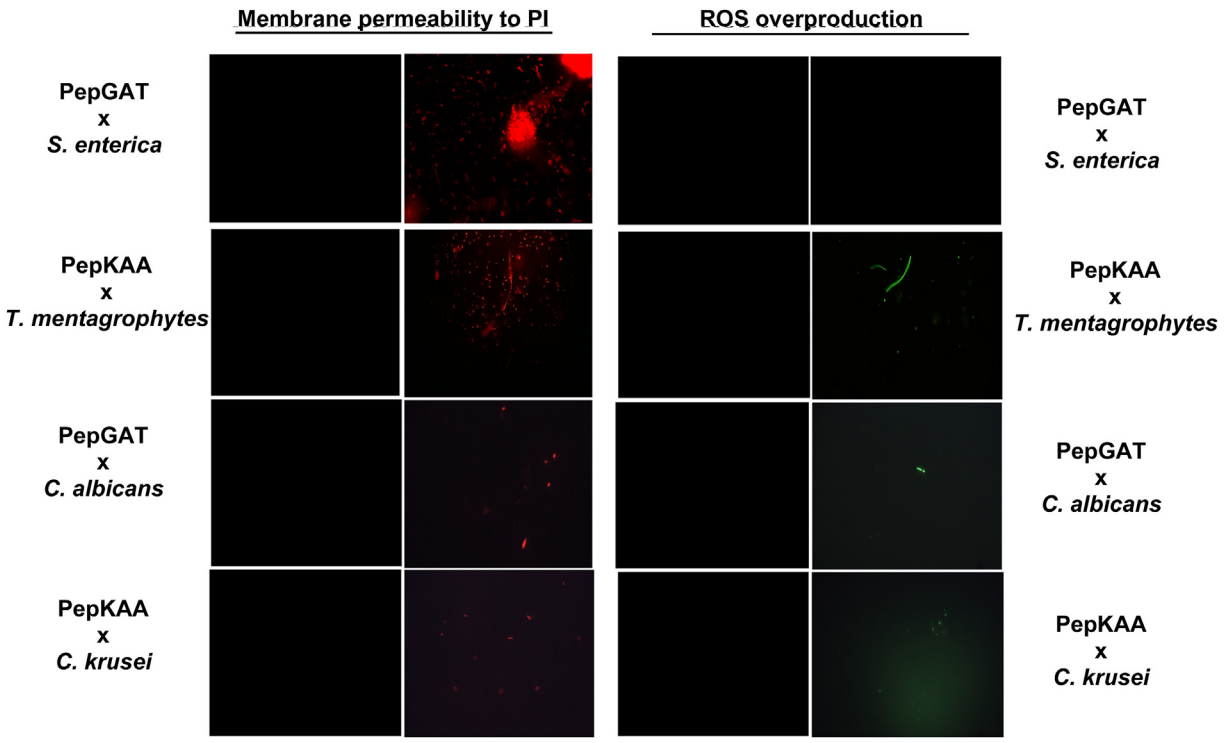

Fig. 4. Fluorescence microscopic analyses showing membrane permeability and ROS overproduction in human pathogens induced by PepGAT and PepKAA. Both peptides were used at 50 μg. mL^{-1}. NaCl-DMSO solution was used as control (left panel). Red fluorescence indicates damage to the membrane by PI uptake and green fluorescence overproduction of ROS (right panel).

Table 4
Antibiofilm activity of synthetic peptides PepGAT and PepKAA.

Microorganisms	Peptides (% of inhibition)				
	Inhibition of Biofilm Formation				
	5% DMSO-0.15 M NaCl	**PepGAT 50 μg mL^{-1}**	**PepKAA 50 μg mL^{-1}**	**Ciprofloxacin[a] 50 μg mL^{-1}**	**Nystatin[b] 50 μg mL^{-1}**
S. enterica	0	0	–	6 ± 0.01	–
C. krusei	0	–	0	–	0
	Degradation of Formed Biofilm				
	5% DMSO-0.15 M NaCl	**PepGAT 50 μg mL^{-1}**	**PepKAA 50 μg mL^{-1}**	**Ciprofloxacin[a] 50 μg mL^{-1}**	**Nystatin[b] 50 μg mL^{-1}**
S. enterica	0	37 ± 0.04	-	22 ± 0.51	–
C. krusei	0	-	40 ± 0.09	–	10 ± 0.03

-Not tested.
[a] Used as positive control to antibacterial assays.
[b] Used as positive control to anticandidal assays.

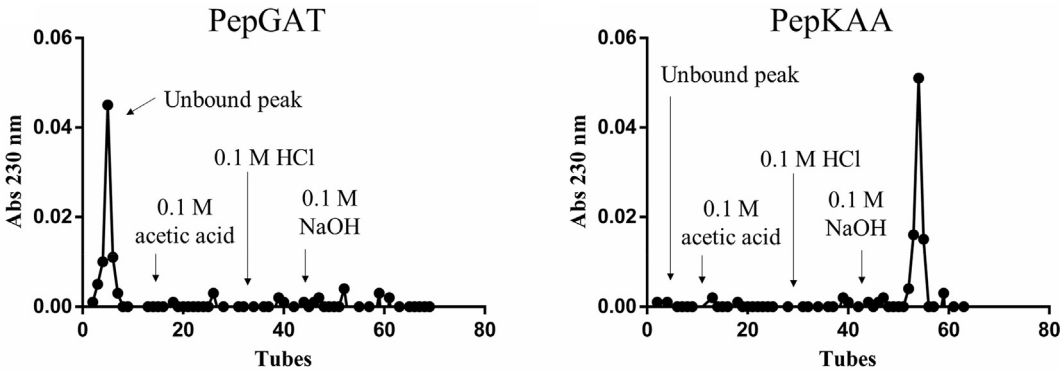

Fig. 5. Affinity chromatography in a chitin column using PepGAT and PepKAA. The column was previously equilibrated with 0.15 M NaCl containing 5% dimethyl sulfoxide (NaCl-DMSO solution). The PepGAT was non-retained and eluted with DMSO-NaCl solution, while the PepKAA was retained in the column and eluted with 0.1 M NaOH.

3.6. Allergenic, toxic and hemolytic potentials and digestibility of peptides

With respect to clinical applications, other important characteristics used to choose the peptides were their allergenic, hemolytic, and toxic potentials. Both PepGAT and PepKAA had no predicted allergenic or toxic potential (Table 2). The bioinformatics analysis also predicted that PepGAT and PepKAA would have very low hemolytic potentials, of 5 and 4%, respectively (Table 2). The *in vitro* hemolytic activity of both peptides was tested against rabbit blood cells (RBC) (Table S4). As expected, 0.1% Triton X-100, used as a positive control for hemolysis, presented 100% hemolysis and the control solutions (5% DMSO, 0.15 M NaCl and a solution of 5% DMSO + 0.15 M NaCl) (peptide vehicle) produced no hemolysis (Table S4). Both peptides were tested at the same concentration that showed antimicrobial activity (50 μg mL^{-1}), and 2, 5, and 10-fold that concentration. None of them presented any signs of hemolysis (Table S4). This result suggests that both peptides are safe to mammalian cells even at concentration 10-fold higher than the antimicrobial activity. For comparison with conventional drugs, hemolysis activity was also assayed with ciprofloxacin (control for bacteria) and nystatin (control for yeasts) at the same concentration as the peptides (Table S4). Ciprofloxacin presented hemolytic activity values of 1.5, 1.5, 8, and 50% at the concentrations of 50, 100, 250, and 500 μg mL^{-1}, respectively, whereas nystatin exhibited 100% hemolysis at all tested concentrations.

The bioinformatics analyses also predicted that both peptides would not be resistant to trypsin digestion due to the presence of arginine residues. With respect to pepsin, PepGAT was predicted to be hydrolyzed at both pH levels tested (pH 1.3 and > 2.0), while PepKAA was predicted to be resistant. Besides this, the stability of the peptides in the intestine-like environment (ILE) was also simulated, with half-lives of 1.115 and 0.879 s, respectively, for PepKAA and PepGAT (Table 2). To test the resistance to *in vitro* digestion, both peptides were incubated in simulated gastric fluid (SGF, pepsin) and simulated intestinal fluid (SIF, pancreatin). PepGAT was readily digested after incubation with SGF and SIF (Fig. 6), since PepGAT ions were not detected in any of the MS spectra obtained afterward. PepKAA remained intact after incubation with SGF for 2 s, 5 min and 2 h, but was digested with SIF at all incubation times (Fig. 7). As predicted, PepKAA was resistant to pepsin digestion, while PepGAT was not (Table 2).

4. Discussion

The rational design of SAMPs based on the sequence of other proteins has been increasing due to many advantages. First, peptides can be designed to improve their potential without side effects [13]. Second, multiple functions can be incorporated in the same peptide sequence [33]. Third, SAMP synthesis is less expensive than some purification processes [14]. Fourth, many online servers facilitate peptide design [9,10]. Fifth, synthetic peptides can be designed to have features that are not present in the proteins used as models [6].

Although many studies have been published reporting SAMPs as potent antimicrobial agents [34,35], none of them provide a workflow either to design or characterize them. Here, we describe a workflow that brings together some servers to clearly and easily design and characterize SAMPs (Fig. 1). First, from a protein sequence, several peptides with antibiofilm and cell-penetrating activities were obtained. Then, those with positive net charge (at least +1), hydrophobic ratio (40–60%), ten amino acids, low Boman index (≤2.5) and α-helix structure were selected and synthetized for further antimicrobial assays.

Following the proposed workflow, we obtained only two peptides (PepGAT and PepKAA) that met all requirements essential for peptides that target the membrane of microorganisms [11]. First of all, a positive charge of peptides is critical to enable them to interact with the negative portion of phospholipids of the membrane by electrostatic forces. Furthermore, the hydrophobic portion of peptides is essential to enable insertion in the membrane's hydrophobic core. The helicity of the peptide and the non-polar face of the α-helix structure are also vital for successful insertion in the membrane and then pore formation [11].

Indeed, to be attracted by the negative charge of the membrane, SAMPs have to present a positive net charge of at least +1. Measuring the correlation between positive charge and activity is difficult, but it is accepted that negative or neutral peptides usually do not have antimicrobial activity. One crucial point to be considered during peptide choice is that a very high positive charge (e.g., > +9) can result in two problems: (1) no antimicrobial activity; and (2) toxicity to mammalian cells [11]. Jiang et al. [36] reported that the reduction of the net charge of V13K to values lower than +4 reduced the antimicrobial activity, whereas increasing values to +8 improved the antimicrobial activity 4-fold. However, analogs of V13K with positive charge higher than +9 not only improved antimicrobial activity but also dramatically increased hemolytic activity.

Following this idea, Lyu et al. [34] reported that PMAP-36 had a net charge of +14 and showed hemolytic activity at 4 μM, whereas its derivative RI12, which had a net charge of +6, only presented hemolytic activity at concentrations >128 μM. Also, Dias et al. [8] produced three synthetic peptides with a net charge of +1. All of them presented antimicrobial activity with no hemolytic effects even at a concentration 128 times higher than the minimum inhibitory concentration (MIC). Altogether, the results showed a correlation between high positive charge (>+9) and hemolytic effects [34,36]. Based on that, PepGAT and PepKAA were chosen because they have net charges of +2 and + 3, respectively.

Both electrostatic and hydrophobic interactions are essential for the antimicrobial activity of SAMPs [11]. Hydrophobicity is necessary for peptides to penetrate the membrane. However, as happens with the charge, high hydrophobic content results in collateral damage such as hemolytic activity. Chen et al. [37] performed a rational design based on the peptide $V13K_L$, which has high hydrophobic content, and found it presented MIC against *P. aeruginosa* and hemolytic activity of 7.8 and 250 μg mL^{-1}, respectively. A less hydrophobic $V13K_L$-derived peptide (L6A/L21A) presented MIC against *P. aeruginosa* and hemolytic activity of >500 and > 1000 μg mL^{-1}, respectively [37]. In addition to the hydrophobic ratio, the hydrophobic moment is also important. Kim et al. [35] reported that by increasing the hydrophobic moment of synthetic peptides, there was a positive correlation with antibacterial activity. For example, Hp1404-T1, with a hydrophobic moment value of 0.699, was 16-fold less efficient to inhibit bacterial growth than Hp1404-T1e, which has a hydrophobic moment value of 0.831. Although both PepGAT and PepKAA presented low values of the hydrophobic moment, respectively, 0.275 and 0.398, they exhibited interesting antimicrobial activity.

The importance of α-helix formation was assessed by Chen et al. [38], who reported that the substitution of L-amino acids with D-amino acids, which only affects α-helix formation, reduced the activity of the peptide. In another work, Lyu et al. [34] designed a peptide (RI18) derived from PAMP-36, an antimicrobial peptide, to improve α-helix formation and stability. The RI18 presented anticandidal activity 8-fold higher than the original peptide, corroborating the importance of α-helix formation for antimicrobial activity. The CD analyses revealed that in aqueous solution, both PepGAT and PepKAA presented a predominance of random coil structure [39]. Both CD spectra slightly changed when peptides

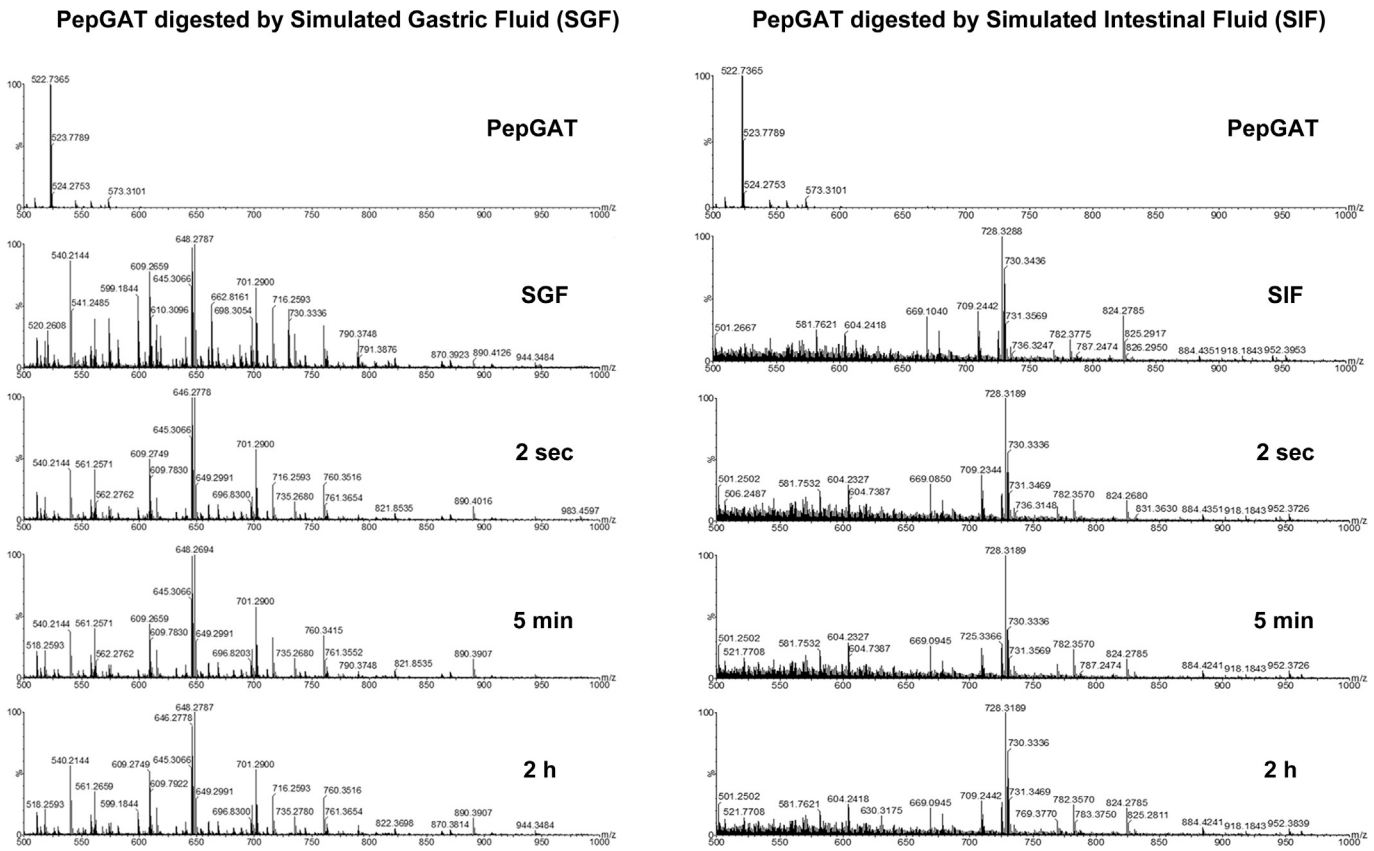

Fig. 6. Mass spectra of PepGAT digested with simulated gastric fluid (SGF) and simulated intestinal fluid (SIF) for 2 s, 5 min, and 2 h.

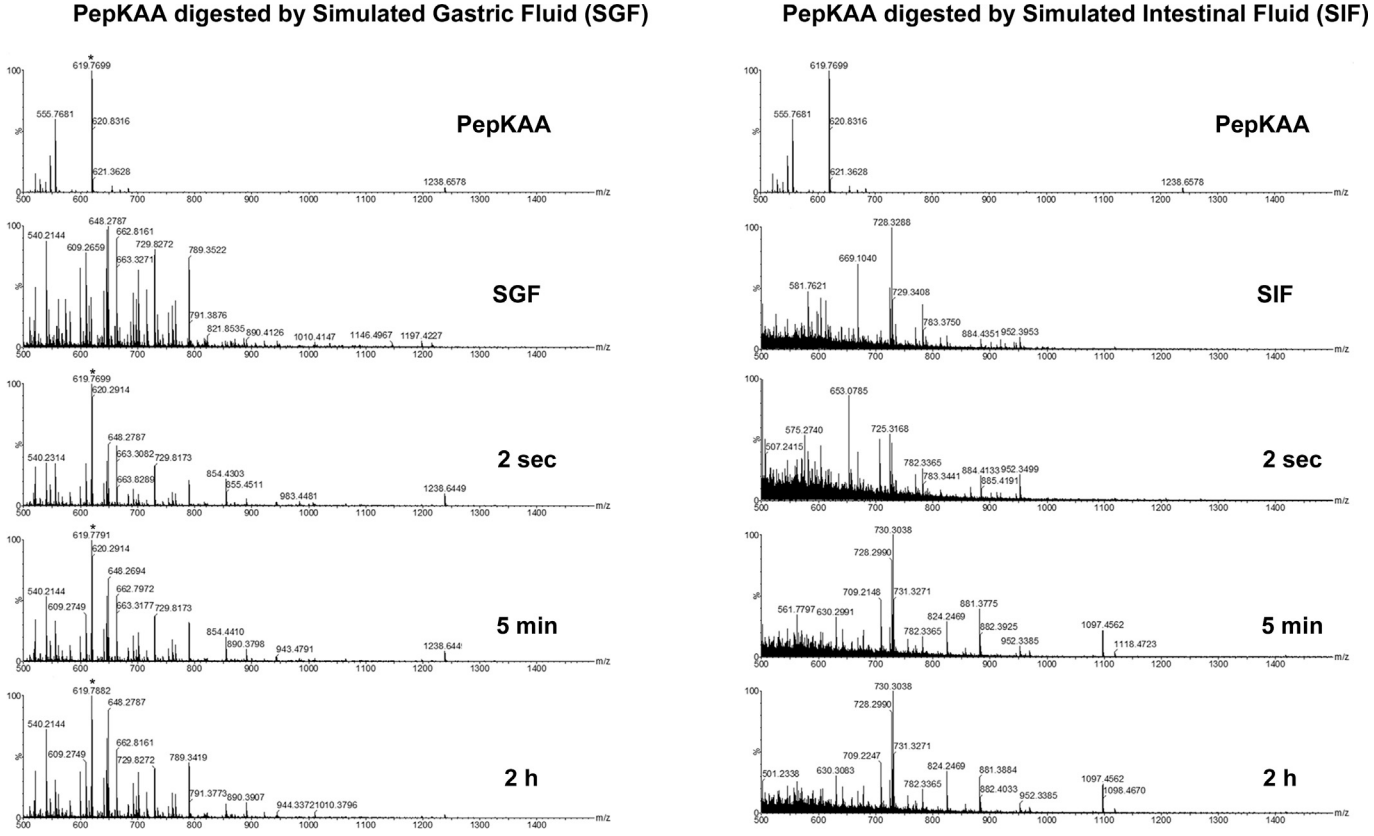

Fig. 7. Mass spectra of PepKAA digested with simulated gastric fluid (SGF) and simulated intestinal fluid (SIF) for 2 s, 5 min, and 2 h.

were in an organic solvent (TFE), which can be attributed to the removal of water molecules from the vicinity of the peptides, favoring intra-chain interactions and resulting in peptide ordering [40]. However, peptides still maintain the characteristic spectra of peptides with random coil structures. It is also noteworthy that both peptides changed their conformation only in the presence of negatively charged membranes (SDS and POPG), like when incubated in TFE. However, this change was more pronounced in PepKAA than PepGAT, suggesting possible selectively of interaction with membrane lipids and thus different antimicrobial activity.

Although it is not the best structure for antimicrobial activity, the random coil structure is still interesting to antimicrobial activity [41]. Su et al. [41] showed that random coil structure in arginine-rich cell-penetrating peptides is essential for rapid translocation across the lipid membrane without causing permanent, but transient, damages to the cell membrane. Accordingly, PepGAT and PepKAA have arginine and random coil structures with the ability to cause membrane damage. Therefore, the low values of the hydrophobic moment and the lack of a stable helical structure can explain the reduced antimicrobial action of both peptides in comparison to well-structured SAMPs.

Using the same approach, Lima et al. [32] correlated the antimicrobial activity of two peptides (*Mo*-CBP$_3$-PepI and *Mo*-CBP$_3$-PepII) with their abilities to interact with SDS micelles. *Mo*-CBP$_3$-PepI, which strongly interacted with the SDS, had higher antimicrobial activity than *Mo*-CBP$_3$-PepII, which did not have a good interaction with the micelles. Besides this, the CD results suggested that PepGAT and PepKAA did not interact with zwitterionic micelles (HPS and POPC). This fact corroborates the absence of hemolytic activity of both peptides, because the erythrocyte plasma membrane is mainly composed of zwitterionic phospholipids [42].

Regarding antibacterial activity, PepGAT was promising against *S. enterica*, which is a very harmful human pathogen, responsible for typhoid fever and non-typhoid infection due to the ingestion of contaminated water and food, leading to over 200,000 deaths annually [43]. Over the years, *S. enterica* has become resistant to many conventional drugs. Therefore, many studies have been focused on *S. enterica*, seeking new alternative treatments based on SAMPs [34,44]. For instance, Tsai et al. [44] reported that at 64 μg mL^{-1}, a synthetic peptide called GWQ4 inhibited *S. enterica* growth by 50% after 48 h, while PepGAT inhibited *S. enterica* growth by 80% at 50 μg mL^{-1} after 24 h. To the best of our knowledge, there is no publication revealing the mechanisms of action of peptides against drug-resistant *S. enterica*, which makes the results shown here more interesting.

By applying AFM and fluorescence microscopy, it was possible to gain some insight into the mechanism of antibacterial activity of PepGAT against *S. enterica*. After 24 h, PepGAT caused *S. enterica* membrane damage, resulting in the inevitable loss of volume and thereby overflow of cytoplasmic content. The damage to the membrane was confirmed by PI uptake, which can only occur when the membrane is damaged, allowing the PI to interact with DNA and thus release red fluorescence [45]. Based on microscopic data, we can suggest that PepGAT targets the *S. enterica* membrane.

Although PepKAA did not show antibacterial activity against the microorganisms tested, it presented strong activity against the dermatophytic fungus *T. mentagrophytes* and the yeast *C. krusei*. *T. mentagrophytes* is an etiological agent of dermatophytosis from the *Trichophyton* genus that has developed resistance to the most common drug used for treatment, griseofulvin [46]. Despite its clinical and economic importance, few published studies have tried to find alternative solutions to fight *T. mentagrophytes* infections. Among the few studies reported, none of them involve proteins or peptides. Most of them have related antifungal action with secondary metabolites, and at extremely high concentrations [47,48]. For instance, to reach 50% inhibition against *T. mentagrophytes*, Lopes et al. [46] needed to use 7800 μg mL^{-1} of phlorotannins. To attain the same inhibition, Rahman et al. [47] employed 500 μg mL^{-1} of essential oil from *Lonicera japonica*. Those concentrations are 156 and 10 times, respectively, higher than the concentration (50 μg mL^{-1}) of PepKAA used to inhibit *T. mentagrophytes* germination by 80%. A major problem associated with the results presented by Lopes et al. [46] and Rahman et al. [47] is the very low purity of the tested compounds, which can result in many collateral effects. Moreover, neither study provided any indications of the action mechanism of these compounds.

SEM analysis revealed the damage caused to the microconidia of *T. mentagrophytes* by treatment with PepKAA. Furthermore, fluorescence analysis of PI uptake confirmed that PepKAA can damage the membrane of microconidia. The ability of PepKAA to induce membrane pore formation in *T. mentagrophytes* makes it a potential synergistic component to conjugate with conventional drugs. For example, the action mechanism of griseofulvin is to inhibit the formation of microtubules. To do that, the drug needs to reach the cytoplasm, which is done by interacting with a membrane transporter [49]. Based on that, PepKAA can improve the action of griseofulvin by producing pore membranes to enable entrance of the drug in the cytoplasm and then inhibition of cytoskeleton formation. In addition to membrane pore formation, PepKAA was able to induce the overproduction of endogenous ROS in *T. mentagrophytes*. The mechanism behind the overproduction of ROS by peptides is still unclear. Nevertheless, it is known that a high level of ROS damages molecules such as DNA and proteins as well as the cell membrane [7].

Related to anticandidal activity, the peptides presented activity only against *C. albicans* and *C. krusei*. However, PepKAA was still more effective, by inhibiting *C. krusei* growth by 80%, whereas PepGAT inhibited *C. albicans* growth by 40%. AFM analysis showed that both peptides induced similar damage to the membrane and cell wall, leading to death of *Candida* cells. Also, by applying SEM analysis, Oliveira et al. [6] demonstrated damage to the candida cell wall after treatment with the synthetic peptide *Mo*-CBP$_3$-PepIII. In addition, those authors reported that *Mo*-CBP$_3$-PepIII had affinity for chitin, exerting action against the cell wall. The PI uptake corroborated the results shown by AFM analysis. By targeting membranes, PepGAT and PepKAA, unlike conventional drugs, which target ergosterol or cell mechanisms (i.e., microtubule formation), hamper the development of resistance because changes in membrane composition can be hazardous and metabolically expensive to cells. The ability to induce pore formation in the membrane is not common to all synthetic peptides, but it seems to be an important mechanism. Lopes et al. [7] and Lyu et al. [34] reported synthetic peptides with anticandidal activity but that were unable to permeate the membrane. Another exciting feature of PepGAT and PepKAA is the ability to induce over-accumulation of ROS in candida cells. Uncontrolled ROS production in cells can be a severe problem, leading to death by damage of important molecules such as DNA, lipids and proteins [7].

Because PepGAT and PepKAA were designed from an antifungal protein (*A. thaliana* chitinase), we expected both peptides to exhibit such activity. However, the bioinformatics analyses and the *in vitro* assays showed that PepGAT was more active against bacteria, whereas PepKAA was better against fungi. These results are very similar to those reported by Dias et al. [8], who found that peptides designed from an antibacterial 2S albumin demonstrated high antifungal activities. Again, these results show a clear advantage of peptide design by incorporating of new function, which was not present in the model protein [33].

Our results show a clear strain-specific activity of PepGAT and PepKAA. The higher activity against dermatophytes and yeasts

displayed by PepKAA can be explained, at least in part, by its affinity for chitin, suggesting that that polymer is the primary target of PepKAA. After binding, the peptide can cross the cell wall and damage the membrane. Accordingly, previous studies have demonstrated the importance of interaction with chitin by antifungal peptides [6,32,50]. For instance, Rogozhin et al. [50] reported that the peptide SmAMP3 presented stronger antifungal activity than SmAMP1, because the first was able to bind to chitin whereas the second was not.

On the other hand, PepGAT was much more active against bacteria than PepKAA. Although both peptides have very similar physicochemical features, they differ in their amino acid composition. PepGAT has two arginine residues and PepKAA has one arginine and two lysine residues. Even though arginine and lysine are positively charged amino acids, the first has a guanidinium side chain, which is responsible for this amino acid being the most hydrophilic found in nature, a feature that has important biological implications [51]. It is known that natural and synthetic AMPs with arginine residues are much more active against bacteria and are better able to penetrate the cell by forming pores in the membrane than those in which lysine is present [52]. In fact, previous studies have shown that the substitution of arginine by lysine leads to a decrease in the antibacterial activity and membrane pore formation ability in tritrpticin, human neutrophil peptide and KR-12 [53–56]. Thus, it is reasonable to suggest that the presence of two arginine residues in PepGAT and only one in PepKAA can be responsible for the differential antibacterial activity between these two peptides.

Finally, PepGAT and PepKAA also demonstrated variable results for different bacteria as well as for different *Candida* spp. The large range of activities against bacteria seems not to be related to the general characteristics between gram-positive and gram-negative bacteria, since PepGAT exhibited high antibacterial activity against *S. enterica* (80% inhibition) but none against *E. aerogenes*, *E. coli* and *P. aeruginosa*, all gram-negative bacteria. Interestingly, PepGAT was active only against *C. albicans* (40% inhibition) and PepKAA against *C. krusei* (80% inhibition). Similarly, a previous study showed that four short peptides designed from porcine myeloid antimicrobial peptide-36 (PMAP-36) were strain-specific against yeasts and bacteria [34]. For instance, RI12 was 8-fold more active against *E. coli* EC183 than against *E. coli* 1005 and *E. coli* 25922. In the same way, the same peptide RI12 was 16-fold more active against *C. tropicalis* than against *C. albicans* [34]. The same authors explained that the results could be due to the differences in cell membrane composition, even in microorganisms of the same species. Thus, although fungi and bacteria have the same general components, the biochemical composition of their cell walls and membranes can be very different, which can explain the selectivity of several antimicrobial peptides. This is very important, because cell-specific molecules can be used, avoiding side-effects and selection for resistant microbes as a consequence of overuse and misuse of these substances.

An important adaptation developed by bacteria and yeasts is the ability to form biofilms. Biofilm formation by microorganisms results in strong antibiotic resistance, which is a global health problem [57]. It is not clear what triggers microorganisms to change from their free forms to biofilms, but it is well known that the extracellular matrix produced during biofilm formation is rich in carbohydrates, proteins, lipids, nucleic acids and water [57]. Biofilms can increase drug resistance 1000-fold to conventional drugs compared to free cells [58]. Here, both peptides were predicted to have antibiofilm activity, which was experimentally confirmed. PepGAT was able to degrade the formed biofilm of *S. enterica* by 37% at 50 μg mL^{-1}. This reduction was 68% higher than that caused by the antibiotic ciprofloxacin, which was 22%. The low effect of antibiotics on biofilms has been reported previously [57]. Zoysa et al. [59] reported a synthetic lipopeptide that inhibited *P. aeruginosa* biofilm by only 25% at 51 μg mL^{-1}. Unlike PepGAT, PepKAA caused 400% more degradation than nystatin, a commercial antifungal drug against *C. krusei* biofilms. At 50 μg mL^{-1}, PepKAA degraded 40% of *C. krusei*, whereas nystatin degraded only 10%.

Besides the impressive activity of PepKAA compared to the commercial antifungal drug, PepKAA's antibiofilm activity was also higher than other synthetic peptides, such as KU4 (96 μg mL^{-1}), uperin 3.6 (96 μg mL^{-1}), upn-lys4 (96 μg mL^{-1}), upn-lys5 (192 μg mL^{-1}), and upn-lys6 (96 μg mL^{-1}), which reduced the viability of *C. albicans* biofilms by 20, 35, 15, 40, and 30%, respectively [60]. In addition, the synthetic peptide VLL-28 at 72 μg mL^{-1} reduced the viability of *C. krusei* biofilms by 35% [61], whereas PepKAA at 1.5-fold lower concentration presented better activity. Recently, Paulone et al. [62] reported a peptide that presented an IC_{50} value against *C. albicans* biofilm of 126 μg mL^{-1}, a concentration almost 3 times higher than that of PepKAA with the same activity.

The in silico approach predicted that PepGAT and PepKAA would present normal and high stability, respectively, in the intestinal environment. Nevertheless, this supposition was not confirmed *in vitro*. Although PepKAA was not digested with SGF, PepGAT was completely digested after 2 s of incubation with SGF and SIF. PepKAA was digested with SIF at all incubation times. The presence of pepsin cleavage sites in the PepGAT explains the digestion in SGF. Probably PepGAT and PepKAA were digested by the various proteases (trypsin, chymotrypsin, elastase and carboxypeptidase) present in the pancreatin mixture (SIF). These results indicate that neither peptide can properly be applied orally. However, both of them can be applied topically, such as in hydrogels or even biomembranes, which can be used against skin infections, because PepKAA presented antifungal activity against the dermatophyte *T. mentagrophytes* and was not allergenic or toxic.

Neither peptide was toxic to rabbit red blood cells even at concentrations 10 times higher than the antimicrobial concentration. This is corroborated by CD analyses, which revealed that neither peptide's structure changed when in contact with zwitterionic membranes, such as erythrocyte membranes. On the other hand, ciprofloxacin was toxic to blood cells only at concentrations 10-fold higher than the antimicrobial activity tested here, whereas nystatin caused 100% hemolysis at all concentrations. Both commercial antibiotics have been reported as hemolytic drugs [63,64]. However, they cause different types of hemolysis. Ciprofloxacin induces autoimmune hemolytic anemia [63] and nystatin causes damage to erythrocyte membranes and hence hemolysis [64]. Despite being potent alternative molecules to treat diseases caused by resistant microbes, many synthetic and natural peptides have presented hemolytic activity [36,37,65]. Jindal et al. [65] reported four potent synthetic antibacterial peptides (RN7-IN10, RN7-IN9, RN7-IN8, and RN7-IN6) that presented MIC_{100} values at 7.81 μg mL^{-1}. On the other hand, those peptides presented high hemolytic and toxic activity against mammalian cells, starting at a concentration 5 times higher than the MIC_{100}. The same happened with the peptide RI21, which presented MIC_{100} against *C. albicans* of 8.6 μg mL^{-1}, while at that same concentration it presented hemolytic activity [34].

5. Conclusion

The pipeline presented here offers an easy step-by-step way to choose, characterize and test potential sequences to be assayed as synthetic antimicrobial peptides. Using this workflow, two peptides (PepGAT and PepKAA) with antimicrobial potential, including activity against biofilms and without any hemolytic effects, were identified and characterized. The results encourage further studies of these peptides to develop new drugs for clinical application.

Funding and acknowledgments

This work was supported by grants from the following Brazilian agencies: Conselho Nacional de Desenvolvimento Científico e Tecnológico (CNPq) (process numbers 308107/2013-6, 304700/2019-3 and 306202/2017-4); Coordenação de Aperfeiçoamento de Pessoal de Nível Superior (CAPES); Fundação de Amparo à Pesquisa do Estado de São Paulo (FAPESP, Grant 2018/19546-7) and Fundação Cearense de Apoio ao Desenvolvimento Científico e Tecnológico (FUNCAP). We are also grateful to the staff of the central analytical facilities of UFC, Brazil.

Author contributions

All authors made substantial contributions in the following steps: (1) the conception and design of the study, or acquisition of data, or analysis, microscopic analysis and interpretation of data were done by PFNS, LSMM, JTAO, PGL, LPD, NASN, FESL, JSS, AFBS, and RFC; (2) JLSL done all the CD experiments and data interpretation; (3) drafting the article or revising it critically with important intellectual content was done by PFNS, AFBS, JLSL, MVR, and CDTF; (4) final approval of the version to be submitted was done by PFNS and CDTF.

Ethical approval

None sought.

Declaration of competing interest

All authors declare no conflict of interest.

Appendix A. Supplementary data

Supplementary data to this article can be found online at https://doi.org/10.1016/j.biochi.2020.05.016.

References

[1] A. Tomasz, Multiple-antibiotic-resistant pathogenic bacteria – A report on the rockefeller university workshop, N. Engl. J. Med. 330 (1994) 1247–1251, https://doi.org/10.1056/NEJM199404283301725.
[2] A.H. Holmes, L.S.P. Moore, A. Sundsfjord, M. Steinbakk, S. Regmi, A. Karkey, P.J. Guerin, L.J. V Piddock, Understanding the mechanisms and drivers of antimicrobial resistance, Lancet 387 (2016) 176–187, https://doi.org/10.1016/S0140-6736(15)00473-0.
[3] M.A. Pfaller, D.J. Diekema, Epidemiology of invasive candidiasis: a persistent public health problem, Clin. Microbiol. Rev. 20 (2007) 133–163, https://doi.org/10.1128/CMR.00029-06.
[4] L.S. Biswaro, M.G.d.C. Sousa, T.M.B. Rezende, S.C. Dias, O.L. Franco, Antimicrobial peptides and nanotechnology, recent advances and challenges, Front. Microbiol. 9 (2018) 855, https://doi.org/10.3389/fmicb.2018.00855.
[5] A. Pfalzgraff, K. Brandenburg, G. Weindl, Antimicrobial peptides and their therapeutic potential for bacterial skin infections and wounds, Front. Pharmacol. 9 (2018) 281, https://doi.org/10.3389/fphar.2018.00281.
[6] J.T.A. Oliveira, P.F.N. Souza, I.M. Vasconcelos, L.P. Dias, T.F. Martins, M.F. Van Tilburg, M.I.F. Guedes, D.O.B. Sousa, Mo-CBP3-PepI, Mo-CBP3-PepII, and Mo-CBP3-PepIII are synthetic antimicrobial peptides active against human pathogens by stimulating ROS generation and increasing plasma membrane permeability, Biochimie 157 (2019) 10–21, https://doi.org/10.1016/J.BIOCHI.2018.10.016.
[7] F.E.S. Lopes, H.P.S. da Costa, P.F.N. Souza, J.P.B. Oliveira, M.V. Ramos, J.E.C. Freire, T.L. Jucá, C.D.T. Freitas, Peptide from thaumatin plant protein exhibits selective anticandidal activity by inducing apoptosis via membrane receptor, Phytochemistry 159 (2019) 46–55, https://doi.org/10.1016/J.PHYTOCHEM.2018.12.006.
[8] L.P. Dias, P.F.N. Souza, J.T.A. Oliveira, I.M. Vasconcelos, N.M.S. Araújo, M.F.V. Tilburg, M.I.F. Guedes, R.F. Carneiro, J.L.S. Lopes, D.O.B. Sousa, RcAlb-PepII, a synthetic small peptide bioinspired in the 2S albumin from the seed cake of Ricinus communis, is a potent antimicrobial agent against Klebsiella pneumoniae and Candida parapsilosis, Biochim. Biophys. Acta Biomembr. (2019) 183092, https://doi.org/10.1016/j.bbamem.2019.183092.
[9] A. Gautam, K. Chaudhary, R. Kumar, G.P.S. Raghava, Computer-Aided Virtual Screening and Designing of Cell-Penetrating Peptides, Humana Press, New York, NY, 2015, pp. 59–69, https://doi.org/10.1007/978-1-4939-2806-4_4.
[10] A. Sharma, P. Gupta, R. Kumar, A. Bhardwaj, dPABBs: a novel in silico approach for predicting and designing anti-biofilm peptides, Sci. Rep. 6 (2016) 21839, https://doi.org/10.1038/srep21839.
[11] Y. Huang, J. Huang, Y. Chen, Alpha-helical cationic antimicrobial peptides: relationships of structure and function, Protein Cell 1 (2010) 143–152, https://doi.org/10.1007/s13238-010-0004-3.
[12] H.G. Boman, buibui, J. Intern. Med. 254 (2003) 197–215, accessed, http://www.ncbi.nlm.nih.gov/pubmed/12930229. (Accessed 2 September 2019).
[13] S. Lata, B.K. Sharma, G. Raghava, Analysis and Prediction of Antibacterial Peptides, 2007, https://doi.org/10.1186/1471-2105-8-263.
[14] S. Lata, N.K. Mishra, G.P. Raghava, AntiBP2: improved version of antibacterial peptide prediction, BMC Bioinf. 11 (2010) S19, https://doi.org/10.1186/1471-2105-11-S1-S19.
[15] X. Lin, S. Kaul, S. Rounsley, T.P. Shea, M.I. Benito, C.D. Town, C.Y. Fujii, T. Mason, C.L. Bowman, M. Barnstead, T.V. Feldblyum, C.R. Buell, K.A. Ketchum, J. Lee, C.M. Ronning, H.L. Koo, K.S. Moffat, L.A. Cronin, M. Shen, G. Pal, S. Van Aken, L. Umayam, L.J. Tallon, J.E. Gill, M.D. Adams, A.J. Carrera, T.H. Creasy, H.M. Goodman, C.R. Somerville, G.P. Copenhaver, D. Preuss, W.C. Nierman, O. White, J.A. Elsen, S.L. Salzberg, C.M. Fraser, J.C. Venter, Sequence and analysis of chromosome 2 of the plant Arabidopsis thaliana, Nature 402 (1999) 761–765, https://doi.org/10.1038/45471.
[16] G. Wang, X. Li, Z. Wang, APD2: the updated antimicrobial peptide database and its application in peptide design, Nucleic Acids Res. 37 (2009), https://doi.org/10.1093/nar/gkn823.
[17] E. Gasteiger, C. Hoogland, A. Gattiker, S. Duvaud, M.R. Wilkins, R.D. Appel, A. Bairoch, Protein identification and analysis tools on the ExPASy server. Proteomics Protoc. Handb., Humana Press, Totowa, NJ, 2005, pp. 571–607, https://doi.org/10.1385/1-59259-890-0:571.
[18] G. Wang, X. Li, Z. Wang, APD3: the antimicrobial peptide database as a tool for research and education, Nucleic Acids Res. 44 (2016) D1087–D1093, https://doi.org/10.1093/nar/gkv1278.
[19] A. Sharma, D. Singla, M. Rashid, G.P. Raghava, Designing of peptides with desired half-life in intestine-like environment, BMC Bioinf. 15 (2014) 282, https://doi.org/10.1186/1471-2105-15-282.
[20] P.K. Meher, T.K. Sahu, A.R. Rao, Prediction of donor splice sites using random forest with a new sequence encoding approach, BioData Min. 9 (2016) 4, https://doi.org/10.1186/s13040-016-0086-4.
[21] M. Molero-Abraham, J.-P. Glutting, D.R. Flower, E.M. Lafuente, P.A. Reche, EPIPOX: immunoinformatic characterization of the shared T-cell epitome between Variola virus and related pathogenic orthopoxviruses, J. Immunol. Res. 2015 (2015) 1–11, https://doi.org/10.1155/2015/738020.
[22] K. Chaudhary, R. Kumar, S. Singh, A. Tuknait, A. Gautam, D. Mathur, P. Anand, G.C. Varshney, G.P.S. Raghava, A web server and mobile app for computing hemolytic potency of peptides, Sci. Rep. 6 (2016) 22843, https://doi.org/10.1038/srep22843.
[23] A. Gautam, P. Kapoor, S. Gupta, K. Chaudhary, G.P.S. Raghava, R. Kumar, In silico approach for predicting toxicity of peptides and proteins, PLoS One 8 (2013), e73957, https://doi.org/10.1371/journal.pone.0073957.
[24] P. Thévenet, Y. Shen, J. Maupetit, F. Guyon, P. Derreumaux, P. Tufféry, PEP-FOLD: an updated de novo structure prediction server for both linear and disulfide bonded cyclic peptides, Nucleic Acids Res. 40 (2012) W288–W293, https://doi.org/10.1093/nar/gks419.
[25] W.L. DeLano, J. Lam, PyMOL, A Communications Tool for Computational Models, 2005.
[26] S.C. Lovell, I.W. Davis, W.B. Arendall, P.I.W. De Bakker, J.M. Word, M.G. Prisant, J.S. Richardson, D.C. Richardson, Structure validation by Cα geometry: ϕ,ψ and Cβ deviation, Proteins Struct. Funct. Genet. 50 (2003) 437–450, https://doi.org/10.1002/prot.10286.
[27] T.D.P. Lopes, P.F.N. Souza, H.P.S. da Costa, M.L. Pereira, J.X. da Silva Neto, P.C. de Paula, R.S.N. Brilhante, J.T.A. Oliveira, I.M. Vasconcelos, D.O.B. Sousa, Mo-CBP4, A purified chitin-binding protein from Moringa oleifera seeds, is a potent antidermatophytic protein: in vitro mechanisms of action, in vivo effect against infection, and clinical application as a hydrogel for skin infection, Int. J. Biol. Macromol. 149 (2020) 432–442, https://doi.org/10.1016/j.ijbiomac.2020.01.257.
[28] M38-A2 Reference Method for Broth Dilution Antifungal Susceptibility Testing of Filamentous FungiApproved Standard, 2008. www.clsi.org.
[29] S.M. Kelly, T.J. Jess, N.C. Price, How to study proteins by circular dichroism, Biochim. Biophys. Acta Protein Proteonomics 1751 (2005) 119–139, https://doi.org/10.1016/j.bbapap.2005.06.005.
[30] A.J. Miles, B.A. Wallace, CDtoolX, a downloadable software package for processing and analyses of circular dichroism spectroscopic data, Protein Sci. 27 (2018) 1717–1722, https://doi.org/10.1002/pro.3474.
[31] C.D.T. Freitas, M.Z.R. Silva, J.P.B. Oliveira, A.F.B. Silva, M.V. Ramos, J.S. de Sousa, Study of milk coagulation induced by chymosin using atomic force microscopy, Food Biosci 29 (2019) 81–85, https://doi.org/10.1016/j.fbio.2019.04.003.
[32] P.G. Lima, P.F.N. Souza, C.D.T. Freitas, J.T.A. Oliveira, L.P. Dias, J.X.S. Neto, I.M. Vasconcelos, J.L.S. Lopes, D.O.B. Sousa, Anticandidal activity of synthetic peptides: mechanism of action revealed by scanning electron and fluorescence microscopies and synergism effect with nystatin, J. Pept. Sci. (2020) 1–13, https://doi.org/10.1002/psc.3249.
[33] J.H. Collier, T. Segura, Evolving the use of peptides as components of

biomaterials, Biomaterials 32 (2011) 4198–4204, https://doi.org/10.1016/j.biomaterials.2011.02.030.
[34] Y. Lyu, Y. Yang, X. Lyu, N. Dong, A. Shan, Antimicrobial activity, improved cell selectivity and mode of action of short PMAP-36-derived peptides against bacteria and Candida, Sci. Rep. 6 (2016) 27258, https://doi.org/10.1038/srep27258.
[35] M.K. Kim, H.K. Kang, S.J. Ko, M.J. Hong, J.K. Bang, C.H. Seo, Y. Park, Mechanisms driving the antibacterial and antibiofilm properties of Hp1404 and its analogue peptides against multidrug-resistant Pseudomonas aeruginosa, Sci. Rep. 8 (2018), https://doi.org/10.1038/s41598-018-19434-7.
[36] Z. Jiang, A.I. Vasil, J.D. Hale, R.E.W. Hancock, M.L. Vasil, R.S. Hodges, Effects of net charge and the number of positively charged residues on the biological activity of amphipathic α-helical cationic antimicrobial peptides, Biopolym. - Pept. Sci. Sect. 90 (2008) 369–383, https://doi.org/10.1002/bip.20911.
[37] Y. Chen, M.T. Guarnieri, A.I. Vasil, M.L. Vasil, C.T. Mant, R.S. Hodges, Role of peptide hydrophobicity in the mechanism of action of alpha-helical antimicrobial peptides, Antimicrob. Agents Chemother. 51 (2007) 1398–1406, https://doi.org/10.1128/AAC.00925-06.
[38] Y. Chen, C.T. Mant, R.S. Hodges, Determination of stereochemistry stability coefficients of amino acid side-chains in an amphipathic alpha-helix, J. Pept. Res. 59 (2002) 18–33, accessed, http://www.ncbi.nlm.nih.gov/pubmed/11906604. (Accessed 10 October 2019).
[39] L. Whitmore, B.A. Wallace, Protein Secondary Structure Analyses from Circular Dichroism Spectroscopy: Methods and Reference Databases, 2007, https://doi.org/10.1002/bip.20853.
[40] P. Luo, R.L. Baldwin, Mechanism of helix induction by trifluoroethanol: a framework for extrapolating the helix-forming properties of peptides from trifluoroethanol/water mixtures back to water, Biochemistry 36 (1997) 8413–8421, https://doi.org/10.1021/bi9707133.
[41] Y. Su, A.J. Waring, P. Ruchala, M. Hong, Membrane-bound dynamic structure of an arginine-rich cell-penetrating peptide, the protein transduction domain of HIV tat, from solid-state NMR, Biochemistry 49 (2010) 6009–6020, https://doi.org/10.1021/bi100642n.
[42] M. Zasloff, Antimicrobial peptides of multicellular organisms, Nature 415 (2002) 389–395, https://doi.org/10.1038/415389a.
[43] J.D. Stanaway, R.C. Reiner, B.F. Blacker, E.M. Goldberg, I.A. Khalil, C.E. Troeger, J.R. Andrews, Z.A. Bhutta, J.A. Crump, J. Im, F. Marks, E. Mintz, S.E. Park, A.K.M. Zaidi, Z. Abebe, A.N. Abejie, I.A. Adedeji, B.A. Ali, A.T. Amare, H.T. Atalay, E.F.G.A. Avokpaho, U. Bacha, A. Barac, N. Bedi, A. Berhane, A.J. Browne, J.L. Chirinos, A. Chitheer, C. Dolecek, M. El Sayed Zaki, B. Eshrati, K.J. Foreman, A. Gemechu, R. Gupta, G.B. Hailu, A. Henok, D.T. Hibstu, C.L. Hoang, O.S. Ilesanmi, V.J. Iyer, A. Kahsay, A. Kasaeian, T.D. Kassa, E.A. Khan, Y.H. Khang, H. Magdy Abd El Razek, M. Melku, D.T. Mengistu, K.A. Mohammad, S. Mohammed, A.H. Mokdad, J.B. Nachega, A. Naheed, C.T. Nguyen, H.L.T. Nguyen, L.H. Nguyen, N.B. Nguyen, T.H. Nguyen, Y.L. Nirayo, T. Pangestu, G.C. Patton, M. Qorbani, R.K. Rai, S.M. Rana, C.L. Ranabhat, K.T. Roba, N.L.S. Roberts, S. Rubino, S. Safiri, B. Sartorius, M. Sawhney, M.S. Shiferaw, D.L. Smith, B.L. Sykes, B.X. Tran, T.T. Tran, K.N. Ukwaja, G.T. Vu, L.G. Vu, F. Weldegebreal, M.K. Yenit, C.J.L. Murray, S.I. Hay, The global burden of typhoid and paratyphoid fevers: a systematic analysis for the Global Burden of Disease Study 2017, Lancet Infect. Dis. 19 (2019) 369–381, https://doi.org/10.1016/S1473-3099(18)30685-6.
[44] W.-C. Tsai, Z.-J. Zhuang, C.-Y. Lin, W.-J. Chen, Novel antimicrobial peptides with promising activity against multidrug resistant Salmonella enterica serovar Choleraesuis and its stress response mechanism, J. Appl. Microbiol. 121 (2016) 952–965, https://doi.org/10.1111/jam.13203.
[45] C.D.T. Freitas, R.O. Silva, M.V. Ramos, C.T.M.N. Porfírio, D.F. Farias, J.S. Sousa, J.P.B. Oliveira, P.F.N. Souza, L.P. Dias, T.B. Grangeiro, Identification, characterization, and antifungal activity of cysteine peptidases from Calotropis procera latex, Phytochemistry (2020) 169, https://doi.org/10.1016/j.phytochem.2019.112163.
[46] I. Weitzman, R.C. Summerbell, The dermatophytes, Clin. Microbiol. Rev. 8 (1995) 240–259, https://doi.org/10.1128/cmr.8.2.240.
[47] G. Lopes, E. Pinto, P.B. Andrade, P. Valentão, Antifungal activity of phlorotannins against dermatophytes and yeasts: approaches to the mechanism of action and influence on Candida albicans virulence factor, PLoS One 8 (2013), https://doi.org/10.1371/journal.pone.0072203.
[48] A. Rahman, S.M. Al-Reza, S.A. Siddiqui, T. Chang, S.C. Kang, Antifungal potential of essential oil and ethanol extracts of Lonicera japonica Thunb. against dermatophytes, EXCLI J 13 (2014) 427.
[49] N.M. Martinez-Rossi, T.A. Bitencourt, N.T.A. Peres, E.A.S. Lang, E.V. Gomes, N.R. Quaresemin, M.P. Martins, L. Lopes, A. Rossi, Dermatophyte resistance to antifungal drugs: mechanisms and prospectus, Front. Microbiol. 9 (2018), https://doi.org/10.3389/fmicb.2018.01108.
[50] E.A. Rogozhin, M.P. Slezina, A.A. Slavokhotova, E.A. Istomina, T.V. Korostyleva, A.N. Smirnov, E.V. Grishin, T.A. Egorov, T.I. Odintsova, A novel antifungal peptide from leaves of the weed Stellaria media L, Biochimie 116 (2015) 125–132, https://doi.org/10.1016/j.biochi.2015.07.014.
[51] K. Hristova, W.C. Wimley, A look at arginine in membranes, J. Membr. Biol. 239 (2011) 49–56, https://doi.org/10.1007/s00232-010-9323-9.
[52] A. Rice, J. Wereszczynski, Probing the disparate effects of arginine and lysine residues on antimicrobial peptide/bilayer association, Biochim. Biophys. Acta Biomembr. 1859 (2017) 1941–1950, https://doi.org/10.1016/j.bbamem.2017.06.002.
[53] L.T. Nguyen, L. De Boer, S.A.J. Zaat, H.J. Vogel, Investigating the cationic side chains of the antimicrobial peptide tritrpticin: hydrogen bonding properties govern its membrane-disruptive activities, Biochim. Biophys. Acta Biomembr. 1808 (2011) 2297–2303, https://doi.org/10.1016/j.bbamem.2011.05.015.
[54] A. Bonucci, E. Balducci, M. Martinelli, R. Pogni, Human neutrophil peptide 1 variants bearing arginine modified cationic side chains: effects on membrane partitioning, Biophys. Chem. 190–191 (2014) 32–40, https://doi.org/10.1016/j.bpc.2014.04.003.
[55] B. Mishra, R.F. Epand, R.M. Epand, G. Wang, Structural location determines functional roles of the basic amino acids of KR-12, the smallest antimicrobial peptide from human cathelicidin LL-37, RSC Adv. (2013), https://doi.org/10.1039/C3RA42599A.
[56] F. Armas, S. Pacor, E. Ferrari, F. Guida, T.A. Pertinhez, A.A. Romani, M. Scocchi, M. Benincasa, Design, antimicrobial activity and mechanism of action of Arg-rich ultra-short cationic lipopeptides, PLoS One 14 (2019), https://doi.org/10.1371/journal.pone.0212447.
[57] C. De La Fuente-Núñez, M.H. Cardoso, E. De Souza Cândido, O.L. Franco, R.E.W. Hancock, Synthetic antibiofilm peptides, Biochim. Biophys. Acta Biomembr. 1858 (2016) 1061–1069, https://doi.org/10.1016/j.bbamem.2015.12.015.
[58] S.A. McEwen, P.J. Collignon, Antimicrobial resistance: a one health perspective, Microbiol. Spectr. 6 (2018), https://doi.org/10.1128/microbiolspec.ARBA-0009-2017.
[59] G.H. De Zoysa, A.J. Cameron, V.V. Hegde, S. Raghothama, V. Sarojini, Antimicrobial peptides with potential for biofilm eradication: synthesis and structure activity relationship studies of battacin peptides, J. Med. Chem. 58 (2015) 625–639, https://doi.org/10.1021/jm501084q.
[60] K.Y. Lum, S.T. Tay, C.F. Le, V.S. Lee, N.H. Sabri, R.D. Velayuthan, H. Hassan, S.D. Sekaran, Activity of novel synthetic peptides against Candida albicans, Sci. Rep. 5 (2015), https://doi.org/10.1038/srep09657.
[61] E. Roscetto, P. Contursi, A. Vollaro, S. Fusco, E. Notomista, M.R. Catania, Antifungal and anti-biofilm activity of the first cryptic antimicrobial peptide from an archaeal protein against Candida spp. clinical isolates, Sci. Rep. 8 (2018), https://doi.org/10.1038/s41598-018-35530-0.
[62] S. Paulone, A. Ardizzoni, A. Tavanti, S. Piccinelli, C. Rizzato, A. Lupetti, B. Colombari, E. Pericolini, L. Polonelli, W. Magliani, S. Conti, B. Posteraro, C. Cermelli, E. Blasi, S. Peppoloni, The synthetic killer peptide KP impairs Candida albicans biofilm in vitro, PLoS One 12 (2017), https://doi.org/10.1371/journal.pone.0181278.
[63] S. Lim, M.G. Alam, Ciprofloxacin-induced acute interstitial nephritis and autoimmune hemolytic anemia, Ren. Fail. 25 (2003) 647–651, https://doi.org/10.1081/JDI-120022557.
[64] A. Knopik-Skrocka, J. Bielawski, The mechanism of the hemolytic activity of polyene antibiotics, Cell. Mol. Biol. Lett. 7 (2002) 31–48, accessed, http://www.ncbi.nlm.nih.gov/pubmed/11944048. (Accessed 29 October 2019).
[65] H.M. Jindal, C. Foh Le, M. Yasim, M. Yusof, R.D. Velayuthan, V.S. Lee, S.M. Zain, D.M. Isa, S.D. Sekaran, Antimicrobial Activity of Novel Synthetic Peptides Derived from Indolicidin and Ranalexin against Streptococcus Pneumoniae, 2015, https://doi.org/10.1371/journal.pone.0128532.